UV patterned nanoporous solid-liquid core waveguides

Gopalakrishnan, Nimi; Sagar, Kaushal Shashikant; Christiansen, Mads Brøkner; Vigild, Martin Etchells; Ndoni, Sokol; Kristensen, Anders

Published in:
Optics Express

Link to article, DOI:
10.1364/OE.18.012903

Publication date:
2010

Document Version
Publisher's PDF, also known as Version of record

UV patterned nanoporous solid-liquid core waveguides

Nimi Gopalakrishnan,[1] Kaushal. S. Sagar,[2] Mads Brøkner Christiansen,[1,*] Martin E. Vigild,[2] Sokol Ndoni,[1] and Anders Kristensen[1]

[1]*Department of Micro and Nanotechnology, Technical University of Denmark, DTU Nanotech, Building 345 East, DK-2800 Kongens Lyngby, Denmark.*
[2]*Department of Chemical and Biochemical Engineering, Technical University of Denmark, DTU Chemical Engineering, Building 423, DK-2800 Kongens Lyngby, Denmark*
mads.christiansen@nanotech.dtu.dk

Abstract Nanoporous Solid-Liquid core waveguides were prepared by UV induced surface modification of hydrophobic nanoporous polymers. With this method, the index contrast (δn = 0.20) is a result of selective water infiltration. The waveguide core is defined by UV light, rendering the exposed part of a nanoporous polymer block hydrophilic. A propagation loss of 0.62 dB/mm and a bend loss of 0.81 dB/90° for bend radius as low as 1.75 mm was obtained in these multimode waveguides.

OCIS codes (160.5470) Polymer; (230.7370) Waveguides.

References and links

1. D. Psaltis, S. R. Quake, and C. Yang, "Developing optofluidic technology through the fusion of microfluidics and optics," Nature **442**(7101), 381–386 (2006).
2. M. P. Duggan, T. McCreedy, and J. W. Aylott, "A non-invasive analysis method for on-chip spectrophotometric detection using liquid-core waveguiding within a 3D architecture," Analyst (Lond.) **128**(11), 1336–1340 (2003).
3. M. Holtz, P. Dasgupta, and G. Zhang, "Small-volume raman spectroscopy with a liquid core waveguide," Anal. Chem. **71**(14), 2934–2938 (1999).
4. H. Schmidt, and A. R. Hawkins, "Optofluidic waveguides I. Concepts and implementations," Microfluidics and Nanofluidics **4**(1–2), 3–16 (2008).
5. A. R. Hawkins, and H. Schmidt, "Optofluidic waveguides II. Fabrication and structures," Microfluidics and Nanofluidics **4**(1–2), 17–32 (2008).
6. A. W. Snyder and J. D. Love, "Total Internal Reflection (TIR)," in *Optical Waveguide theory*, (Chapman and Hall, London, 1983)
7. H. Takiguchi, A. Tsubata, M. Miyata, T. Odake, H. Hotta, T. Umemura, and K. Tsunoda, "Liquid core waveguide spectrophotometry for the sensitive determination of nitrite in river water samples," Anal. Sci. **22**(7), 1017–1019 (2006).
8. P. Measor, L. Seballos, D. Yin, J. Z. Zhang, E. J. Lunt, A. R. Hawkins, and H. Schmidt, "On-chip surface-enhanced Raman scattering detection using integrated liquid-core waveguides," Appl. Phys. Lett. **90**(21), 211107 (2007).
9. V. Korampally, S. Mukherjee, M. Hossain, R. Manor, M. Yun, K. Gangopadhyay, L. Polo-Parada, and S. Gangopadhyay, "Development of a Miniaturized Liquid Core Waveguide System With Nanoporous Dielectric Cladding-A Potential Biosensing Platform," IEEE Sens. J. **9**(12), 1711–1718 (2009).
10. W. Risk, H. Kim, R. Miller, H. Temkin, and S. Gangopadhyay, "Optical waveguides with an aqueous core and a low-index nanoporous cladding," Opt. Express **12**(26), 6446–6455 (2004), http://www.opticsinfobase.org/oe/abstract.cfm?URI=oe-12-26-6446.
11. S. Ndoni, M. E. Vigild, and R. H. Berg, "Nanoporous materials with spherical and gyroid cavities created by quantitative etching of polydimethylsiloxane in polystyrene-polydimethylsiloxane block copolymers," J. Am. Chem. Soc. **125**(44), 13366–13367 (2003).
12. M. Hansen, M. Vigild, R. Berg, and S. Ndoni, "Nanoporous crosslinked polyisoprene from polyisoprene - Polydimethylsiloxane block copolymer," Polym. Bull. **51**(5–6), 403–409 (2004).
13. F. Guo, J. W. Andreasen, M. E. Vigild, and S. Ndoni, "Influence of 1, 2-PB matrix cross-linking on structure and properties of selectively etched 1, 2-PB-b-PDMS block copolymers," Macromolecules **40**(10), 3669–3675 (2007).
14. S. Ndoni, C. M. Papadakis, F. S. Bates, and K. Almdal, "Laboratory-scale setup for anionic-polymerization under inert atmosphere," Rev. Sci. Instrum. **66**(2), 1090–1095 (1995).
15. S. Ndoni, L. Li, L. Schulte, P. P. Szewczykowski, T. W. Hansen, F. Guo, R. H. Berg, and M. E. Vigild, "Controlled Photooxidation of Nanoporous Polymers," Macromolecules **42**(12), 3877–3880 (2009).
16. J. E .Mark, in *Polymer data handbook*, (Oxford University Press, New York, 1999)

#127743 - $15.00 USD Received 3 May 2010; revised 27 May 2010; accepted 28 May 2010; published 1 Jun 2010

17. C. Adam, J. Lacoste, and J. Lemaire, "Photo-oxidation of elastomeric materials Part IV–Photo-oxidation of 1,2-polybutadiene," Polym. Degrad. Stabil. **29**(3), 305–320 (1990).
18. I. Papakonstantinou, K. Wang, D. R. Selviah, and F. A. Fernández, "Transition, radiation and propagation loss in polymer multimode waveguide bends," Opt. Express **15**(2), 669–679 (2007), http://www.opticsinfobase.org/oe/abstract.cfm?URI=oe-15-2-669.
19. S. Musa, A. Borreman, A. A. M. Kok, M. B. J. Diemeer, and A. Driessen, "Experimental study of bent multimode optical waveguides," Appl. Opt. **43**(30), 5705–5707 (2004).
20. P. Steinvurzel, B. Kuhlmey, T. White, M. Steel, C. de Sterke, and B. Eggleton, "Long wavelength anti-resonant guidance in high index inclusion microstructured fibers," Opt. Express **12**(22), 5424–5433 (2004), http://www.opticsinfobase.org/oe/abstract.cfm?URI=oe-12-22-5424.
21. A. E. Vasdekis, G. E. Town, G. A. Turnbull, and I. D. W. Samuel, "Fluidic fibre dye lasers," Opt. Express **15**(7), 3962–3967 (2007), http://www.opticsinfobase.org/oe/abstract.cfm?URI=oe-15-7-3962.
22. R. Manor, A. Datta, I. Ahmad, M. Holtz, S. Gangopadhyay, and T. Dallas, "Microfabrication and characterization of liquid core waveguide glass channels coated with Teflon AF," IEEE Sens. J. **3**(6), 687–692 (2003).
23. C. L. Bliss, J. N. McMullin, and C. J. Backhouse, "Integrated wavelength-selective optical waveguides for microfluidic-based laser-induced fluorescence detection," Lab Chip **8**(1), 143–151 (2007).
24. D. Yin, H. Schmidt, J. P. Barber, E. J. Lunt, and A. R. Hawkins, "Optical characterization of arch-shaped ARROW waveguides with liquid cores," Opt. Express **13**(26), 10564–10570 (2005), http://www.opticsinfobase.org/oe/abstract.cfm?URI=oe-13-26-10564.
25. D. Qi, and A. J. Berger, "Chemical concentration measurement in blood serum and urine samples using liquid-core optical fiber Raman spectroscopy," Appl. Opt. **46**(10), 1726–1734 (2007).

1. Introduction

Optofluidics combine optics and fluidics, opening new frontiers in developing optical systems that exploit fluidic properties [1] and analyse the properties of fluids [2,3]. Integration of liquid and optical elements on the same platform is essential for a more compact and robust optofluidic device [4,5]. Liquid-Core waveguides (LCW) confine light and liquid in the same volume providing large interaction length and reduced sample volume. Highly sensitive optofluidics devices can be designed using LCWs. Total internal reflection (TIR) [6] techniques are usually employed to guide light in the LCWs. As water or aqueous solutions ($n \approx 1.33$) forms the core of LCW, the major challenge is in finding a suitable solid cladding material with refractive index below 1.33. Most applied technologies in this field include Teflon AF cladded LCWs [7], Anti Resonant Reflecting Optical Waveguides (ARROWs) [8] and nanoporous clad LCWs [9,10]. Although Teflon AF is widely used, low surface energy and inertness to chemical functionalization present challenges to use this material in planar chip fabrication.

This work presents nanoporous waveguides, consisting of a clad of hydrophobic nanoporous polymer (NP) and a core of hydrophilic NP infiltrated by liquid. The typical pore size (14 nm) and spacing of the nanoporous polymer is significantly smaller than the wavelength of guided light. Therefore, the core of our waveguides is a solid-liquid 'alloy', hence an appropriate acronym for these waveguides would be Solid-Liquid Core Waveguides (SLCW). We also report losses (propagation, bending and coupling loss) observed in these waveguides studied with cutback techniques.

2. Device fabrication

An attractive way to obtain NP polymers is by total or partial removal of one block from self-assembled block copolymers. The morphology of the self-assembled material is determined by the block's volume fraction in block copolymers and by thermodynamical variables [11–13]. In our work, the starting material is a self-assembled diblock copolymer of Polybutadiene and Polydimethylsiloxane (PB-PDMS) [Fig. 1(a)]. PB-PDMS was synthesized by anionic polymerization [14]. The schematic illustration of the working principle of SLCW in 1,2 Polybutadine (PB) nanoporous polymers is shown in Fig. 1. NP polymers were prepared initially by solvent casting the PB-PDMS block copolymer in tetrahydrofuran (THF) with 1 mol % of the cross-linker dicumyl peroxide with respect to the number of double bonds of the PB component. The morphology of the self assembly determines the distribution of pores in the polymer matrix. The material was further cross-linked at 140°C in an argon/nitrogen atmosphere for 2 hours in order to provide mechanical stability to the PB

#127743 - $15.00 USD Received 3 May 2010; revised 27 May 2010; accepted 28 May 2010; published 1 Jun 2010

matrix. A volume fraction of 0.60 for the PB block in the original block polymer was controlled by the polymer synthesis and the obtained self-assembled morphology was of the cubic symmetry $Ia\bar{3}d$, known also as gyroid morphology [11,15]. This morphology provides bicontinuous porosity and high transparency, which are important for the liquid transport and for waveguiding characteristics of the obtained device. The cross-linked PB-PDMS block copolymer was rendered nanoporous by selectively etching the PDMS minority block from the bulk system, using tetrabutyl ammonium fluoride (TBAF) at three times molar excess, relative to the repeating unit of PDMS. Etching took 36 h and was followed by cleaning of the PB matrix in THF and methanol for a total of 16 h. A porosity of 0.44 [Fig. 1(b)] was determined by methanol uptake [13] from the obtained material. The volume fraction of cross-linked PB (0.56) is lower than that of the uncrosslinked PB (0.60) due to increase of density induced by cross-linking.

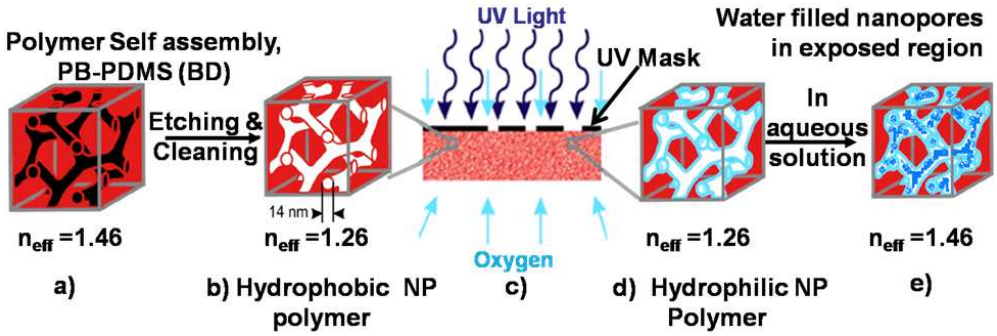

Fig. 1. Schematic illustration of working principle of Liquid Core waveguiding n 1,2-PB nanoporous polymers (a) Polymer self assembly of PB-PDMS, (b) Minority block etched hydrophobic NP polymer, (c) Selectivity UV exposure using a UV mask in presence of oxygen, (d) Hydrophillic NP polymer formed at exposed regions, (e) Exposed region infiltrated with water have changed effective refractive index.

The self-assembled block copolymer and the nanoporous polymer obtained from it can be considered as binary alloys with heterogeneity length scale much lower than the wavelength of visible light. An effective refractive index n_{eff} of the block copolymer or NP can be calculated by the Lorentz-Lorenz relation

$$\frac{n_{eff}^2 - n_1^2}{n_{eff}^2 + 2} = V_2 \frac{n_2^2 - n_1^2}{n_2^2 + 2}, \qquad (1)$$

where n_1, n_2 are the refractive indices of the matrix and the minory component respectively, and V_2 is the volume fraction of the minority component (PDMS or air). In the NP polymer, PDMS minority block (n_2 = 1.40) [16] is replaced with air (n_2 = 1). Thus a 44% porosity (V_2 = 0.44) induces an n_{eff} change from 1.46 for the block copolymer to 1.26 for the NP [Fig. 1(b)]. Photo oxidation [17] in the presence of UV light (300-350 nm) changes the surface wetting property of the naturally hydrophobic 1,2-PB NP polymer [13]. The resultant hydroxyl and carboxyl groups on the matrix air interface, render the exposed region hydrophilic [Fig. 1(c), 1(d)]. On immersion in aqueous solution, water infiltrates the pores in the exposed regions, increasing its effective refractive index (δn_{eff} = 0.20). The index mismatch obtained was exploited to confine light within the solid-liquid core [Fig. 1(e)]. Water evaporation does happen from the surface of the porous waveguide on a timescale of 10-15 minutes. This does not affect our experiments, which are done much faster, and in the future, when we expect to add a cladding, this should further minimize evaporation. When the waveguides dry they seize to guide light. To verify water infiltration we used an organic fluorescent dye (Rhodamine 6G), in aqueous solution. These molecules are smaller than the pores, and thus they infiltrate the exposed regions. As the index mismatch induced is governed by the liquid infiltration of

#127743 - $15.00 USD Received 3 May 2010; revised 27 May 2010; accepted 28 May 2010; published 1 Jun 2010

nanopores, the liquid core will always confine light in these systems. For instance, even if the initial NP polymer (owing to less porosity) had a n_{eff} >1.33, the liquid filled NP region (solid-liquid core) will always have an effective index of refraction higher than the cladding material. We call this type of waveguide a nanoporous solid-liquid core waveguide, shortly NP SLCW or simply SLCW.

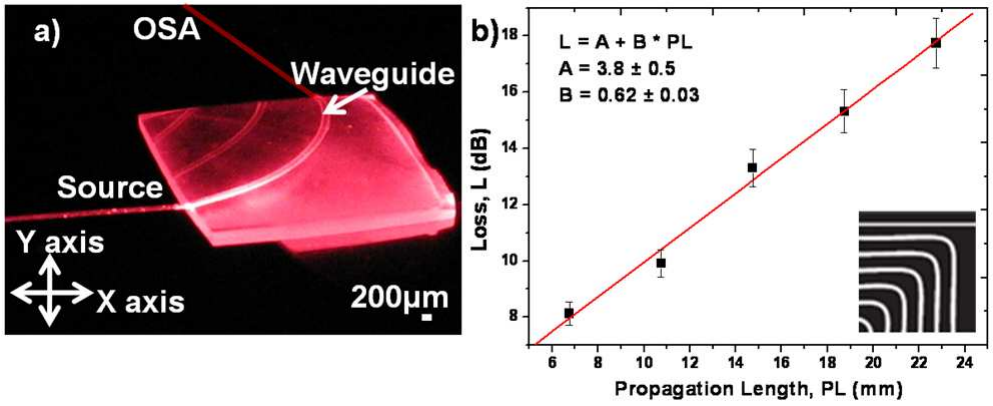

Fig. 2. (a) Experimental setup for measuring propagation and bend loss in the NP LCW, (b) Loss (L) in waveguides with different lengths as a function of propagation length (PL). The solid curve is a linear fit to the measured data. (Inset) 1.5 × 1.5 cm UV mask designed for measuring propagation loss in NP polymer LCW.

3. Results and discussions

The SLCWs were characterized by measuring the losses in the waveguide. Four types of losses occur in rectangular waveguides with bends: input and output coupling, transition, radiation and propagation loss [18,19]. Since the shape of the waveguide is not optimized we have chosen not to focus on transition and coupling losses. Transition losses depend on the waveguide design, e.g. when changing from a curved to a straight section. This can be minimized in the design phase, but cannot be avoided completely in any integrated system. Coupling losses from outside the chip might be an issue, especially if water evaporates from the ends [20,21]. We have not experienced water evaporation causing bubbles, perhaps due to the nanoporous nature of our cladding. Evaporation from the ends is not more pronounced than from the sides in our case.

In this work, propagation loss in 1,2-PB SLCW was studied using the cutback technique. Waveguides of cross section 200 × 200μm were defined with UV patterning using lithography masks as shown in Fig. 2(b). A He-Ne laser (632.8nm) was butt coupled into the SLCW using a 62.5/125μm multimode (MM) fiber. The output from the waveguide was collected with similar MM fibers into an Optical Spectrum Analyser (OSA) (Ando AQ-6315A). The experimental setup is shown in Fig. 2(a). Each waveguide was designed with a 90° bend of radius R = 2mm sandwiched between straight waveguides of varying length. The loss in straight waveguide was obtained by subtracting the loss from 90° bend waveguide of radius, R = 2mm. This removes the coupling and radiation losses. The propagation loss was evaluated by plotting straight waveguide loss as a function of propagation length [Fig. 2(b)]. A linear fit [straight line in Fig. 2(b)] to the data, gives the propagation losses in these waveguides. The constant A [Fig. 2(b)] represents the transition losses when light propagates through different types of waveguides (straight and bend). A transition loss of 3.8 ± 0.5dB and a propagation loss of 0.62 ± 0.03 dB/mm were obtained in the NP SLCWs.

Bending loss evaluation was carried out on waveguides with 90° bend of different bend radius ranging from 1.75 to 11.75 mm. Each of the bend waveguides were sandwiched between 2mm long straight waveguides. The total loss in the bend region was plotted as a function of bend radii in Fig. 3. The loss is obtained by removing coupling and propagation

#127743 - $15.00 USD Received 3 May 2010; revised 27 May 2010; accepted 28 May 2010; published 1 Jun 2010

losses from the straight waveguide section in the design. Transition loss, propagation loss and radiation loss in the bend waveguides were interpreted by fitting a polynomial to the data. The intercept A1 partially indicates transition losses in the waveguide while the linear coefficient B1 contributes to propagation and radiation losses. Each bend waveguide has a propagation length of $(\pi/2) \times R$, (bend radius). Thus the B1 coefficient in Fig. 3 would be expected to be $\pi/2$ times larger than the B coefficient from Fig. 2. That it is somewhat larger in this case is attributed to fabrication differences. With increasing bend radius, a bend waveguide has longer propagation length and lesser degree of bend. This reduces the radiation loss in the waveguide, giving more prominence to propagation losses. The magnitude of the total loss for large bend waveguides is in good agreement with losses from straight waveguides of similar length. |B2| corresponds to the radiation losses in these waveguides.

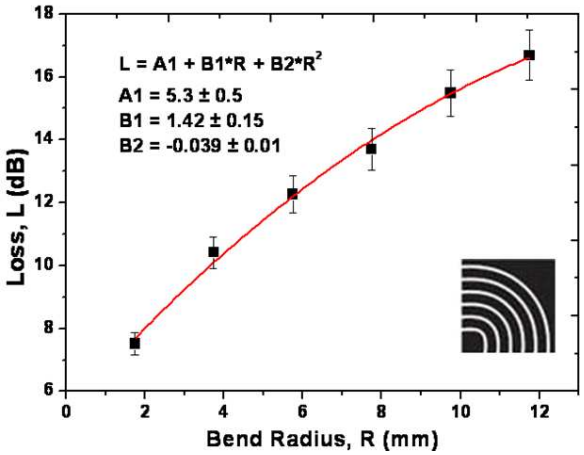

Fig. 3. Total loss (L) is plotted as a function of bend radius (R) for 90° bend waveguides. The solid curve is a polynomial fit to the measured data. (Inset) 1.5 × 1.5 cm UV mask designed with 90° bend waveguides with different bend radii ranging from 1.75 to 11.75 mm.

Since |B2| is very small, propagation loss dominates in our device designs. In NP LCW devices, bend loss of 0.81 dB/90° bend for a small bend radius of 1.75 mm was observed. In the current work, the optimum coupling and transition loss is not discussed. Even with present loss values compared with Teflon AF 2400 waveguides (loss = 0.03 dB/mm) [22], UV modified NP materials could be an alternative for LCW. As typical lengths of optofluidic devices in detection systems are of order of centimeters, high surface area for functionalization and high numerical aperture (NA = 0.74) make UV modified NP a very viable material. In comparison with other types of LCWs [23,24], NP SLCW currently have slightly higher losses. We anticipate that with improved lithography techniques and optimization the losses in these waveguides can be reduced due to smoother surfaces. Optimized lithography should also make it possible to define single mode waveguides. It is also noted that our fabrication technique enables tuning of the index contrast, which can be minimized to lower the number of supported modes.

4. Conclusion

We have illustrated the working principle behind NP SLCWs, where the waveguide core is defined by UV induced hydrophilization of a nanoporous polymer matrix. A quantitative analysis of losses observed in these devices has also been performed. With SLCWs, the major challenges faced in liquid core waveguiding technology can be addressed, in particular simple fabrication and the possibility of having an effective core index above that of the analyte. In addition to the refractive index tuning flexibility, these systems have very high surface area. If the surface is chemically functionalized the interaction between optical field and analyte bound to the surface is vastly enhanced compared to a conventional liquid core waveguide.

#127743 - $15.00 USD Received 3 May 2010; revised 27 May 2010; accepted 28 May 2010; published 1 Jun 2010

Light and water confinement in the same microchannel as well as nanoporosity makes NP SLCWs very promising devices for new applications in optofluidics [25].

Acknowledgments

The financial support of the LiCorT Project by the Danish Council for Strategic Research (grant no. 09-063776/DSF) is gratefully acknowledged. Mads Brøkner Christiansen is financially supported by the Danish Research Council for Technology and Production Sciences (grant no. 274-09-0105)

#127743 - $15.00 USD Received 3 May 2010; revised 27 May 2010; accepted 28 May 2010; published 1 Jun 2010